Published in final edited form as:

Nat Biotechnol. 2015 October ; 33(10): 1073–1075. doi:10.1038/nbt.3357.

Sub-angstrom single-molecule measurements of motor proteins using a nanopore

Ian M Derrington[1], **Jonathan M Craig**[1], **Eric Stava**[2], **Andrew H Laszlo**[1], **Brian C Ross**[1], **Henry Brinkerhoff**[1], **Ian C Nova**[1], **Kenji Doering**[1], **Benjamin I Tickman**[1], **Mostafa Ronaghi**[2], **Jeffrey G Mandell**[2], **Kevin L Gunderson**[2], and **Jens H Gundlach**[1]

[1]University of Washington, Department of Physics, Seattle, Washington

[2]Illumina Inc., San Diego, California

Abstract

Present techniques for measuring the motion of single motor proteins, such as FRET and optical tweezers, are limited to a resolution of ~300 pm. We use ion current modulation through the protein nanopore MspA to observe translocation of helicase Hel308 on DNA with up to ~40 picometer sensitivity. This approach should be applicable to any protein that translocates on DNA or RNA, including helicases, polymerases, recombinases and DNA repair enzymes.

The ability to directly observe the molecular motion of single molecules in real-time provides insights that are not feasible with bulk assays. To date, the highest-precision single-molecule measurements have been obtained using optical tweezers, which can measure motor protein procession with ~300 p.m. spatial resolution at ~1 ms time scales[1,2]. Here we present single-molecule picometer-resolution nanopore tweezers (SPRNT), a method for monitoring the motion and conformational changes of processive nucleic-acid-binding proteins as the nucleic acid passes through a nanopore. SPRNT detects nucleic acid motion relative to the enzyme that processes it with a precision of ~40 p.m. on timescales shorter than a millisecond. We use SPRNT to observe two distinct sub-states in the ATP hydrolysis cycle of a helicase.

SPRNT draws upon the concept of nanopore DNA sequencing[3]. In nanopore sequencing, a nanometer-sized pore is formed between two chambers filled with an ionic solution (Fig. 1a, Supplementary Fig. 1). Upon application of an electrostatic field, an ion current flows

Correspondence should be addressed to J.H.G. (jens@phys.washington.edu).

Author Contributions

I.M.D., J.M.C., E.S., A.H.L, I.C.N, J.G.M., K.L.G. and J.H.G. designed experiments. J.M.C., H.B, I.C.N, K.D and B.I.T. performed the research. I.M.D., J.M.C., E.S., A.H.L., B.C.R., H.B and J.H.G. analyzed the data. I.M.D., J.M.C., A.H.L, J.H.G wrote the paper. K.L.G. and J.H.G. led the research teams.

Competing Financial interests statement:

M.R., J.G.M., and K.L.G. declare competing financial interests in the form of stock ownership and paid employment by Illumina, Inc. J.H.G. is a paid part-time consultant for Illumina. One or more embodiments of one or more patents and patent applications filed by UW and Illumina may encompass the methods, reagents, and the data disclosed in this manuscript. Some work in this study is related to technology described in patent applications.

through the pore and draws single stranded DNA (ssDNA) into the pore. The presence of DNA nucleotides in the pore's constriction modulates the ion current. A motor enzyme is used to move the ssDNAthrough the pore at speeds of 1–100 nt/s, thereby enabling the ion current to be correlated with the DNA sequence[4,5]. Here we use a mutated *Mycobacterium smegmatis* porin A (MspA)[6] which has a short narrow constriction capable of resolving individual DNA nucleotides (Fig. 1b)[4,7]. We find that the exquisite base sensitivity of MspA allows for precise measurement of the position of the DNA inside the pore and thereby enables study of the motion of DNA through processive enzymes. Such measurements can be used to infer conformational changes of enzymes and kinetic stepping parameters. Figure 1c shows raw ion current data. Each current level represents a single nucleotide (nt) step of the motor enzyme phi29 DNA polymerase along the DNA strand and the current magnitude corresponds to the sequence of the DNA passing through the pore's constriction (Fig. 1d)[4,7]. Each level can be resolved with sub millisecond accuracy and pico ampere precision (Supplementary Fig. 2).

For some sequence contexts there is a large change in ion current when the DNA moves by one nucleotide. The ion current levels associated with a sequence of DNA containing an abasic site (marked by an "X") has a change in current equal to ~16 pA when the DNA moved by one nucleotide (Fig. 1e). If the DNA were to move within MspA by a distance of about one tenth of a nucleotide, a linear interpolation would have the observed current change by about one tenth of the change in current, or approximately 1.6 pA. Coupling the ion-current to the DNA position allows us to measure the position of DNA in MspA to precision much smaller than one nucleotide. The scale in Fig. 1e, which shows the conversion of current to displacement, uses a cubic spline to approximate the ion current between levels measured at 1 nt intervals. Using this distance scale we relate the uncertainty of ion current levels to the uncertainty of the DNA position in the pore. For the ion current levels depicted in Fig. 1e a position uncertainty as small as 0.06 nt can be resolved, corresponding to a distance uncertainty of ~40 p.m.[§]. § We assume an inter-phosphate distance to be 690 p.m[8,9]. and 88–95% DNA-elongation.

Next, we changed the elongation of DNA by altering the electrostatic force applied to the DNA. Whilst DNA was moved by phi29 DNAP in single nucleotide steps, we applied driving potentials of 140 mV and 180 mV. Changing the voltage (and thereby the force on the DNA) alters the elongation of DNA between the motor enzyme and pore constriction and shifts the position of nucleotides within MspA's constriction (Fig. 1f). Figure 1g displays the levels for data taken at the two voltages with cubic spline interpolants overlaid. The location of the splines' peaks shift between the different voltages. After normalizing the current amplitudes, we find that the spline for levels taken at 180 mV can predict the levels at 140 mV, when the spline is shifted 0.29 ± 0.03 nt (Fig. 1g). Exploring DNA elongation with voltages between 100 mV and 200 mV indicated that the DNA elongation was consistent with experimental force-stretching curves for ssDNA[8,9] for forces in the range ~20–40 pN (Supplementary Fig. 3, Supplement Discussion 1). These results show that the spline is a reasonable prediction of currents between levels seen at 1 nt intervals.

We evaluated the precision of SPRNT using Hel308, which is an ATP-dependent Ski2-like superfamily II (SF2) helicase/translocase that unwinds duplex DNA in the 3′ to 5′ direction.

Hel308 is conserved in many archaea and eukaryotes, including humans[10]. With a known crystal structure, Hel308 is a good system for understanding processive SF2 helicases[11]. We used Hel308 of *Thermococcus gammatolerans* EJ3 (Accession # YP_002959236.1) (hereafter Hel308).

The current patterns we observed were qualitatively similar to those observed with phi29 DNAP (Fig. 2a,b). However, when Hel308 moved DNA through the pore, we observed nearly twice the number of levels as compared to when phi29 DNAP moved DNA through the pore even though the same length of DNA passed through the pore (Fig. 2a,b).

By comparing 72 Hel308 DNA translocation events, we produced a consensus set of current levels for Hel308 DNA translocations of DNA "sequence A" through the pore (Fig. 2c, 2d, Supplementary discussion 2, Supplementary Figs. 4–5). We used this consensus set to deduce the position of DNA when Hel308 controlled DNA translocation compared with the position of the same DNA sequence moved by phi29 DNAP (Fig. 2a, Online methods). We found that the odd numbered Hel308 current levels correspond to the DNA being held 0.14 ± 0.03 nt *higher* in the pore than the closest corresponding current level taken with phi29 DNAP. We found the even numbered Hel308 levels correspond to the DNA being held 0.41 ± 0.03 nt *lower* in the pore. The average difference in position between the odd and even numbered Hel308 steps is therefore 0.55 ± 0.04 nt. (Additional data are presented in Supplementary discussion 2, Supplementary Fig. 6.)

Next, we examined the median duration ($\tau_{½}$) of each level at different ATP concentrations (Fig. 2e, Supplementary Discussion 3). In Fig. 2f we compare the median duration of each current level at 10 μM ATP to those at 1 mM ATP by dividing $\tau_{½}$ (10 μM) by $\tau_{½}$ (1 mM); we found that the durations for even numbered levels (unshaded) depend on [ATP] while durations for odd numbered levels (shaded) are independent of [ATP]. The ion current magnitude did not change with [ATP]. A full [ATP] titration is described and shown in Supplmenental discussion 4 and Supplementary Figs. 7–9.

Büttner *et al.'s* analysis of the crystal structures of Hel308 and the SF2 helicase, Vasa, revealed large conformational shifts upon ATP binding[11]. Büttner *et al.*[11] propose an inchworm model in which the two RecA-fold DNA binding domains, through the action of ATP binding and then hydrolysis, take turns moving along a DNA strand. In SPRNT the movement of the DNA in the MspA pore is likely a combination of the movement of DNA inside Hel308 and conformational changes of the Hel308 that reposition Hel308 on the MspA rim (thereby changing the position of DNA inside the pore; Supplementary Fig. 10a). Even so, our observations seem to confirm the model predicted by Büttner *et al.* Using Büttner's model[11], we suggest that motif IV within domain 2 pushes the DNA upwards toward domain 1 upon ATP binding, thereby pushing the DNA partially upward within the pore (Supplementary Fig. 10b,c). ATP hydrolysis and ADP release finishes the hydrolysis cycle advancing the DNA and finishing the single nucleotide step. Previously, sub-state kinetic steps have only been inferred indirectly through fitting of durations in helicase systems[12]. However, to our knowledge, no other real-time single molecule method has allowed direct observation of sub-states within individual hydrolysis cycles of helicase kinetics.

To maximize SPRNT's resolution, it is important to choose DNA sequences that produce current levels with large differences (not homopolymeric sequences). The current between full nucleotide steps may differ from the spline interpolation that we used. Finally, during SPRNT, MspA is in contact with the enzyme and applies a 20 to 50 pN force to the enzyme (Supplementary discussion 1). These forces and contact with MspA may alter the enzyme's activity.

In addition to its sub-angstrom resolution, SPRNT simultaneously provides the exact location of the enzyme along the DNA sequence[7]. This means that SPRNT could be used to answer important questions in many motor enzyme systems such as how nucleic acid sequence and structure relate to pausing and other motor enzyme activity[13]. SPRNT can resolve smaller motions of enzyme subdomains than FRET and could be used with DNA and RNA polymerases or translocases, a ribosome, or transcription complexes. Other potential applications include analyzing reactive molecules tethered to a polymer (DNA, RNA, or hybrids) that is held in the pore

Materials and Methods (Online)

Proteins

The M2-NNN-MspA protein[6] was custom ordered from GenScript. Wild-type phi29 DNAP (833,000 U/ml; specific activity 83,000 U/mg) was obtained from Enzymatics or Epicenter. Hel308 was expressed using standard techniques by in-house facilities. Both phi29 DNAP and Hel308 were stored at −20 °C until immediately before use.

DNA constructs

DNA oligonucleotides were synthesized at Stanford University Protein and Nucleic Acid Facility and purified at their facility using column purification methods. The oligo sequences are shown in Supplement Table 1. For both phi29 DNAP and Hel308 experiments, the nanopore read the same sequences for DNA threaded 5′ first. For phi29 DNAP experiments, sequences were previously used in Refs4،14. In particular, DNA templates, primers and blocking oligomers were mixed at relative molar concentrations of 1:1:1.2 and annealed by incubating at 95 °C for 3 min followed by slow-cooling to below 30 °C.

To promote loading of Hel308 onto the template DNA strand, we annealed the template to a complement primer such that the template strand had an eight base 3′ overhang (Supplementary Fig. 11, Supplement Table 1). A 5′ cholesterol on the complement strand promoted the DNA binding to the bilayer, and increased the interaction rate of DNA with the pore[15]. In solution, Hel308 binds to the 3′ overhang on the template strand and may begin to unwind the dsDNA in the 5′ direction. The 5′ end of the template DNA strand is drawn into the pore by the voltage, causing the complement strand to dissociate[16]. Hel308 bound to the DNA prevents complete translocation of the template strand through MspA[17]. Hel308 then functions as a translocase, drawing the ssDNA out of the nanopore in the 3′ direction back into the *cis* well. Supplemental Fig. 3 illustrates the DNA translocase activity of DNA of through MspA by Hel308. We recorded >2000 current traces in various conditions, demonstrating enzymatic movement along DNA (Supplement Table 2). With 180 mV

applied, the currents were higher with Hel308 than with Phi29 DNAP because the buffer contained higher [KCl].

For Hel308 helicase unwinding experiments we used DNA that would promote Hel308 unwinding dsDNA, after the template ssDNA was drawn into the pore. The template strand was constructed with a 5′ cholesterol tail to facilitate insertion of the DNA into the bilayer and a free 3′ end to be drawn into the pore. Two complementary strands were annealed to the template on either side of four adjacent 3-carbon spacers on the template strand. One complement strand, called the decoy, was annealed so that there was a 16 base 3′ overhang on the template strand on which the helicase loaded. In solution Hel308 unwinds the double-stranded decoy complement, but did not efficiently translocate past the 3-carbon spacers. When drawn into the pore, the voltage pulls the 3-carbons spacers through Hel308 to the second complement strand. Hel308 then unwinds the remaining double-stranded complement section, which allowed us to view the unwinding of dsDNA by viewing the single stranded template processed through the pore in the 3′ direction. In this case the DNA is translocated the same direction the voltage gradient pulls the DNA. Supplemental Fig. 10 illustrates the DNA helicase activity of DNA of through MspA by Hel308.

Operating Buffers

For phi29 DNAP experiments we used buffers of 300 mM KCl or asymmetric 150 mM *cis* KCl and 500 mM *trans* KCl, both with 10 mM HEPES at pH 8.0, 1 mM EDTA, 1 mM DTT and 10mM $MgCl_2$. For Hel308 we used buffer at 400 mM KCl with 10 mM HEPES at pH 8.0, 1 mM EDTA, 1 mM DTT, and 10 mM $MgCl_2$. Buffer [KCl] was higher than for phi29 DNAP experiments because the helicase operated better in higher salinity conditions.

Nanopore experiments

The experiments containing single M2-NNN MspA nanopores were established using thoroughly established techniques[6,18]. In short, we formed a lipid bilayer with 1,2-diphytanoyl-sn-glycerol-3- phosphocholine (Avanti Polar Lipids) across a horizontal ~20 μμ diameter aperture separating two ~60 μL chambers containing our operating buffers. (Supplementary Fig. 1). An Axopatch 200B or Axopatch 1B integrating patch clamp amplifier (Axon Instruments) applied a 180 mV voltage (unless otherwise noted) across the bilayer (*trans* side positive) and measured the ionic current through the pore. M2-NNN MspA was added to the grounded *cis* compartment to a final concentration of ~2.5 ng/ml. Once a single pore inserted, as seen by a characteristic increase in the conductance, the buffer was replaced with MspA-free buffer to prevent additional pore formation. The DNA was added to the *cis* compartment to a final concentration of 10 nM. In a standard Phi29 DNAP experiment dCTP, dATP, dTTP and dGTP was added at the final concentrations of 100μM and Phi29 DNAP was added to a final concentration 20nM. In standard Hel308 experiments, our buffers of 400 mM KCl were premade with varying concentrations of ATP (10 μM, 20 μM, 50 μM, 250 μM, 500 μM, 1 mM, 3 mM). 1 mL of the chosen premixed solution was perfused into the *cis* chamber, ensuring the uniform concentration of ATP. In the Hel308 experiments, DNA was added to a final concentration of 10 nM and Hel308 to a final concentration of 100 nM. Unless otherwise mentioned, experiments were done at room temperature (23 ± 1 °C).

Measurement of DNA position for Hel308 experiments

After scaling Hel308 levels and positioning them relative to the levels previously measured with phi29 DNAP, we found that all Hel308 levels lie along a spline interpolant between the phi29 DNAP current levels (Fig. 2c). Odd numbered Hel308 levels are close to previously observed phi29 DNAP current levels. Even numbered Hel308 levels lie along the interpolant somewhere in-between previously measured levels. As above in Fig. 2d, we found the position of both the even and odd numbered Hel308 levels relative to the levels taken with phi29 DNAP.

Data acquisition and analysis

Data was acquired at 50 kHz with acquisition software written in LabView (National Instruments). Current traces were analyzed using custom programs written in Matlab (The MathWorks), Java and C. Collected data were box-filtered with at 10 point window and down-sampled to 5.0 kHz. DNA interactions and enzyme motor events were detected using previously described algorithms[4,6,7,14,19]. Ion current levels were selected automatically using the level finding algorithm used in Ref7. using elements of the level finder more thoroughly described in Schreiber *et al.*[20]. Event counts and statistics are summarized in Supplementary Table 2. Additional methods can be found in the Supplementary Discussions 1–4.

Supplementary Material

Refer to Web version on PubMed Central for supplementary material.

Acknowledgments

This work was supported at University of Washington by National Institute of Health, NHGRI grant R01HG005115 and at Illumina through internal funding. We thank Josh J. Bartlett, Samuel Klebanoff, Mark T. Svet, and Matthew T. Noakes for assisting in the data collection and Cheng-Yao Chen, Ali Nikoomanzar and Weihua Chang for making Hel308 and testing its activity. Matthew Hopper, Nicholas Sam-Soon and Sinduja Marx performed the initial experiments that revealed Hel308's fractional steps and their ATP dependence.

References

1. Ha T, Kozlov AG, Lohman TM. Single-molecule views of protein movement on single-stranded DNA. Annu. Rev. Biophys. 2012; 41:295–319. [PubMed: 22404684]
2. Kim H, Ha T. Single-molecule nanometry for biological physics. Rep. Prog. Phys. 2013; 76:016601. [PubMed: 23249673]
3. Kasianowicz JJ, Brandin E, Branton D, Deamer DW. Characterization of individual polynucleotide molecules using a membrane channel. Proc. Natl. Acad. Sci. USA. 1996; 93:13770–13773. [PubMed: 8943010]
4. Manrao EA, et al. Reading DNA at single-nucleotide resolution with a mutant MspA nanopore and phi29 DNA polymerase. Nat. Biotechnol. 2012; 30:349–353. [PubMed: 22446694]
5. Cherf GM, et al. Automated forward and reverse ratcheting of DNA in a nanopore at 5-Å precision. Nat. Biotechnol. 2012; 30:344–348. [PubMed: 22334048]
6. Butler TZ, Pavlenok M, Derrington IM, Niederweis M, Gundlach JH. Single-molecule DNA detection with an engineered MspA protein nanopore. Proc. Natl. Acad. Sci. USA. 2008; 105:20647–20652. [PubMed: 19098105]
7. Laszlo AH, et al. Decoding long nanopore sequencing reads of natural DNA. Nat. Biotechnol. 2014; 32:829–833. [PubMed: 24964173]

8. Smith SB, Cui Y, Bustamante C. Overstretching B-DNA: the elastic response of individual double-stranded and single-stranded DNA molecules. Science. 1996; 271:795–799. [PubMed: 8628994]
9. Bosco A, Camunas-Soler J, Ritort F. Elastic properties and secondary structure formation of single-stranded DNA at monovalent and divalent salt conditions. Nucleic Acids Res. 2014; 42:2064–2074. [PubMed: 24225314]
10. Woodman ILB, Bolt EL. Winged helix domains with unknown function in Hel308 and related helicases. Biochem. Soc. Trans. 2011; 39:140–144. [PubMed: 21265761]
11. Büttner K, Nehring S, Hopfner K-P. Structural basis for DNA duplex separation by a superfamily-2 helicase. Nat. Struct. Mol. Biol. 2007; 14:647–652. [PubMed: 17558417]
12. Myong S, Bruno MM, Pyle AM, Ha T. Spring-loaded mechanism of DNA unwinding by hepatitis C virus NS3 helicase. Science. 2007; 317:513–516. [PubMed: 17656723]
13. Herbert KM, Greenleaf WJ, Block SM. Single-molecule studies of RNA polymerase: motoring along. Annu. Rev. Biochem. 2008; 77:149–176. [PubMed: 18410247]
14. Laszlo AH, et al. Detection and mapping of 5-methylcytosine and 5-hydroxymethylcytosine with nanopore MspA. Proc. Natl. Acad. Sci. USA. 2013; 110:18904–18909. [PubMed: 24167255]
15. Adam, G.; Delbruck, M. Reduction of dimensionality in biological diffusion processes. In: Rich, A.; Davidson, N., editors. Structural Chemistry and Molecular Biology. W.H. Freeman & Co.; 1968. p. 198-215.
16. Mathé J, Visram H, Viasnoff V, Rabin Y, Meller A. Nanopore unzipping of individual DNA hairpin molecules. Biophys. J. 2004; 87:3205–3212. [PubMed: 15347593]
17. Henrickson SE, Misakian M, Robertson B, Kasianowicz JJ. Driven DNA transport into an asymmetric nanometer-scale pore. Phys. Rev. Lett. 2000; 85:3057–3060. [PubMed: 11006002]
18. Akeson M, Branton D, Kasianowicz JJ, Brandin E, Deamer DW. Microsecond time-scale discrimination among polycytidylic acid, polyadenylic acid, and polyuridylic acid as homopolymers or as segments within single RNA molecules. Biophys. J. 1999; 77:3227–3233. [PubMed: 10585944]
19. Derrington IM, et al. Nanopore DNA sequencing with MspA. Proc. Natl. Acad. Sci. USA. 2010; 107:16060–16065. [PubMed: 20798343]
20. Schreiber JM, Karplus K. Segmentation of noisy signals generated by a nanopore. bioRxiv. 2015 http://biorxiv.org/content/early/2015/01/23/014258.

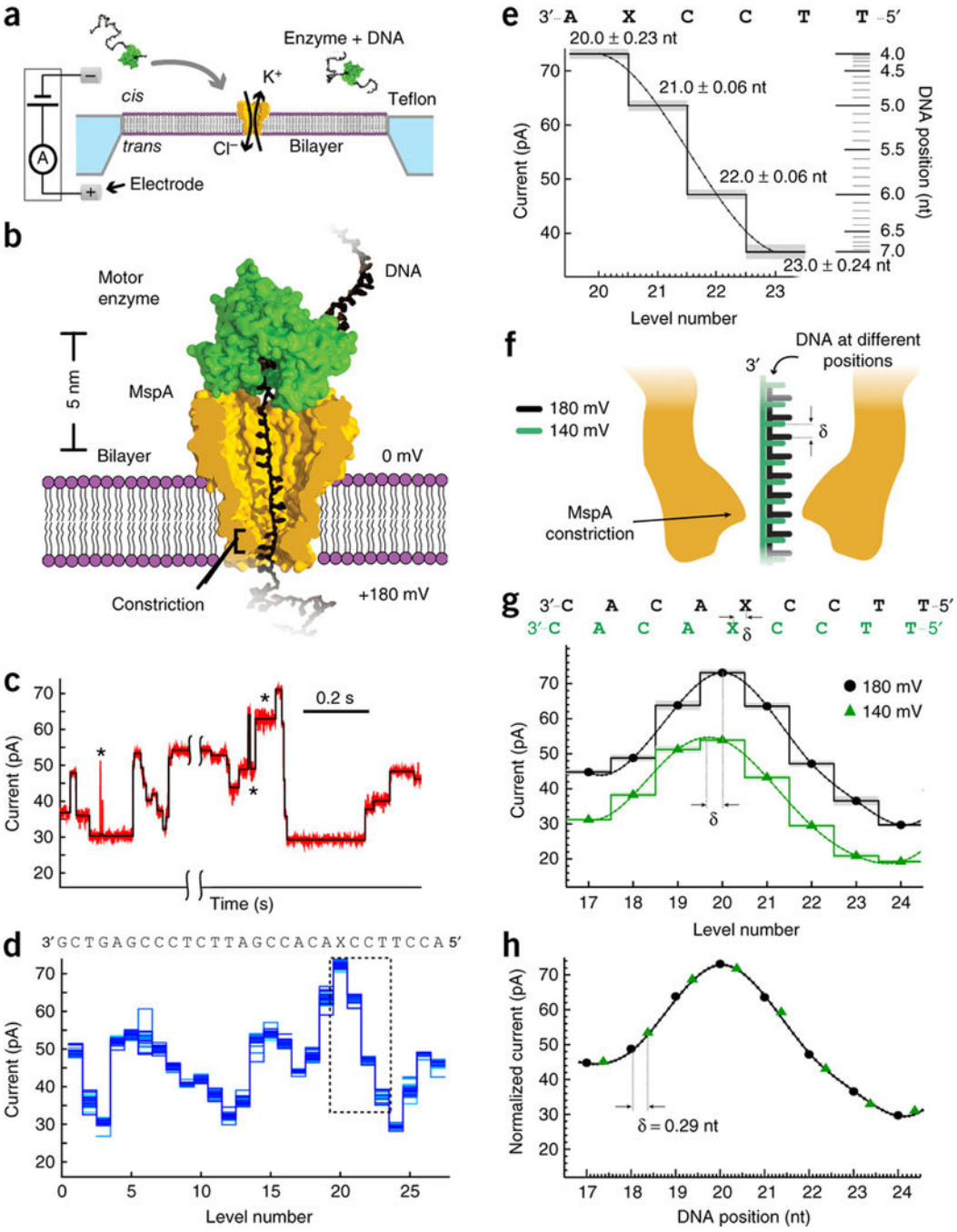

Figure 1. The nanopore system

(a) A phospholipid lipid bilayer (purple) spans a Teflon (light blue) aperture, separating a KCl solution into *cis* and *trans* compartments. A single MspA nanopore (gold) is inserted into the bilayer. A voltage applied via two Ag/AgCl electrodes causes ion current through the pore. The electric potential also attracts enzyme-DNA complexes into the pore (green and black; not to scale). **(b)** ssDNA bound to the motor enzyme (polymerase or helicase) threads through the pore's constriction until the enzyme comes to rest on the pore rim. The enzyme controls the DNA's motion through the pore, while the nucleotides positioned

within MspA's constriction govern the ion current. **(c)** The phi29 DNA polymerase (DNAP) moves the DNA through MspA in single-nucleotide steps resulting in distinct current levels. Black lines mark the average current of observed levels. Breaks in the current trace are for current levels lasting more than 200 ms. Back-stepping of the phi29 DNAP causes repetitions of levels, indicated by *. **(d)** The mean ion current of the time-ordered levels and overlay the pattern of current levels for 31 recordings of the same sequence of DNA. The associated DNA sequence is shown; 'X' is an abasic residue. **(e)** Zoomed in view of the dashed box in (d) demonstrates conversion of current measurement to DNA position using a smooth curve (spline) fit to the current pattern. The standard deviation translates to uncertainty in DNA position is as low as 0.06 nt. **(f)** Illustration showing that lower voltage, i.e. decreased force, reduces the DNA's elongation and shifts its position within MspA's constriction. **(g)** Comparison of ion current levels recorded at 180 mV (black circles) and at 140 mV (green triangles). Peaks of the spline interpolation illustrate a shift of the DNA's position. **(h)** Current values for 180 mV (black circles) and a spline interpolation to those levels (black curve). Green triangles show the current levels taken at 140 mV in panel (c) after applying a multiplicative scale and additive current offset. The scaled 140 mV levels were horizontally displaced by $\delta = 0.29$ nt to put them in line with the 180 mV spline. "Level number" refers to the number assigned to each level as it appears in order while "DNA position" refers to the position of DNA within the pore. We define integer DNA positions to be identical to phi29 DNAP level numbers.

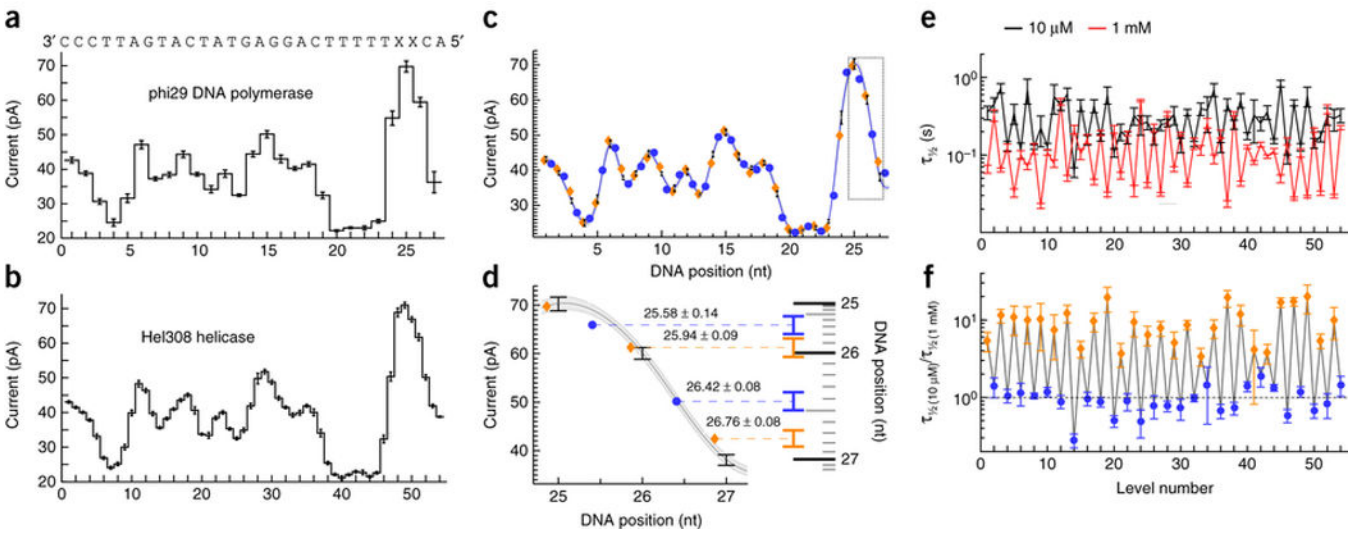

Figure 2. SPRNT applied to the helicase Hel308

(a) Consensus of current level patters for 20 reads of DNA "sequence A" with phi29 DNAP controlling DNA translocation through the pore. **(b)** Same as in a except for 72 reads using Hel308 to control the DNA motion. **(c)** Means of current levels recorded with Hel308 actuated DNA movement (orange and blue symbols) scaled to match a spline (grey curve) of the levels found with phi29 DNAP-controlled movement (black points), also shown in (a). The shaded levels in (b), indicated with orange diamonds, were similar to levels found with phi29 DNAP but were horizontally offset by −0.14 nt in order to best match the spline of levels taken with phi29 DNAP. The unshaded levels in (b), indicated with blue circles, were offset by + 0.41 nt relative to the single nucleotide step positions taken by phi29 DNAP. **(d)** Expanded view of DNA positions 25 through 27, with colors indicating the same elements as (c). As in Figures 1e, h, we illustrate the use of the spline of the phi29-DNAP levels as a distance scale to find the position of even and odd numbered levels found with Hel308 (Supplemental Discussion 2). **(e)** Median duration of corresponding current levels in (b) for two different ATP concentrations: 10 µM (blue) and 1 mM (red) ATP. The median duration of shaded levels is dependent on [ATP]. **(f)** The ratio of the median durations with high and low [ATP] removes sequence dependence that also influences the step durations (Supplemntal discussion 4). The levels alternate between ATP-independent levels (marked with blue dots) and ATP-dependent levels (marked with orange diamonds).